

# A Novel Magnetostrictive Curvature Sensor Employing Flexible, Figure-of-Eight Sensing Coils

G. Moreton, T. Meydan, and P. Williams

Wolfson Centre for Magnetics, School of Engineering, Cardiff University, Cardiff CF24 3AA, U.K.

The demand for accurate angle measurements in a form that is robust and small is high, due to the advances in virtual reality applications, primarily the virtual reality headsets. The peripheral devices are required to completely immerse the user in a virtual reality setting, and for this purpose, a robust sensor has been developed. The angle measurements can also be used in motion sensing applications for medical purposes, allowing monitoring of a patient's condition. This paper presents the development of a planar figure-of-eight coil sensor, which has been designed for the purpose of curvature sensing. The copper-plated polyimide material, FR4 FLEX, was used for the fabrication of the planar figure-of-eight coil. A curvature sensor was designed and consists of the figure-of-eight coil along with the magnetostrictive material Metglas 2605SA1. The sensor was incorporated in an oscillator circuit, where curvature-induced stress within the material changes the amplitude and the frequency of the output signal of the circuit.

*Index Terms*—Curvature sensor, magnetostrictive, planar coils.

## I. INTRODUCTION

MOTION sensing is a key aspect for a fully immersive virtual reality experience, and there are existing methods, which can be used to a high degree of accuracy to capture and detect motion; however, these are often cumbersome [1]. Motion sensing also plays an important role in medical assessments, especially in determining the progress of certain treatments. Wearable motion sensors have been used extensively for medical applications, for the measuring of many different parameters ranging from cardiac rhythms to limb movements [1]–[5]. There is a demand for sensors that are convenient to use and easy to implement, particularly in the development of new sensors, which are suited for usage as part of a wearable device.

A wearable curvature sensor utilizing the inverse magnetostrictive effect has been designed and tested. The sensor has many advantages over the traditional curvature sensors; it can be miniaturized for applications, such as finger motion tracking, an important parameter for virtual reality, and medical purposes. The miniaturization of the sensor can be achieved by the fabrication of the sensor, an operation which can be increased and reduced in scale. Etching techniques [6], [7] have been used for the fabrication of extremely thin sensors, and other techniques, such as printing [8], [9], also produce sensors, which share similar characteristics to those created by etching.

The design of the sensor is based on a planar figure-of-eight coil layer, with a stress sensitive magnetostrictive layer on top. The sensor is a composite device containing both ribbon and polyimide flexible layers, so both parts of the sensor bend; however, the sensor's output is only affected by bending stresses in the ribbon. This particular configuration allows for very small sensors to be produced. There are currently many

sensor applications for the figure-of-eight configuration, as the coil design can be exploited to produce flat coils, minimizing the size of both excitation and pickup coils [10], [11]. This design has been configured to have two coils, which spirals out from the center, and this is to produce a planar coil with the figure-of-eight design.

## II. EXPERIMENTAL METHODS

The sensor coils were drafted using DesignSpark, a printed circuit board (PCB) prototyping software. Preliminary coil designs were milled on solid PCB boards with Metglas ribbon placed on top. This was to test the feasibility of detecting inductance changes due to the close proximity of a magnetostrictive ribbon being stressed. The sensor coil was attached to an  $LC$  tank oscillator, and the output signal of the oscillator would vary as the stresses applied to the material varied. The difference in frequency and amplitude was the most noticeable. The final coil design chosen had 50 turns in total, 25 in each half, with a gap separating the two halves. The gap separating the coils ensures that there is no resistance to motion at the joints, which will be located at the center of the sensor. It also simplifies the calculation of the bending angle.

The material used for the finished sensor was copper clad FR4 FLEX, which consists of a flexible polyimide layer sandwiched between two copper layers. Standard etching techniques were used to transfer the coil design (Fig. 1) on to the top copper layer, and this process is summarized in the flowchart of Fig. 2. The coils were treated with an insulation spray before the magnetostrictive ribbon was attached on top using adhesive tape, thus completing the final sensor assembly (Fig. 3). Copper tracks are  $63.5 \mu\text{m}$  in thickness, and the thickness of the insulation is negligible.

For the experiment, the planar copper coil was combined with as-cast Metglas ribbon 2605SA1 as an inductor in an  $LC$  tank, which is then incorporated as part of a Colpitts oscillator. The changes to the permeability of the magnetostrictive ribbon,  $\mu_r$ , caused a difference in both the frequency and the amplitude of the output signal, and this is due to

Manuscript received September 7, 2015; revised December 22, 2015; accepted January 12, 2016. Corresponding author: T. Meydan (e-mail: meydan@cardiff.ac.uk).

Color versions of one or more of the figures in this paper are available online at <http://ieeexplore.ieee.org>.

Digital Object Identifier 10.1109/TMAG.2016.2520828

This work is licensed under a Creative Commons Attribution 3.0 License. For more information, see <http://creativecommons.org/licenses/by/3.0/>

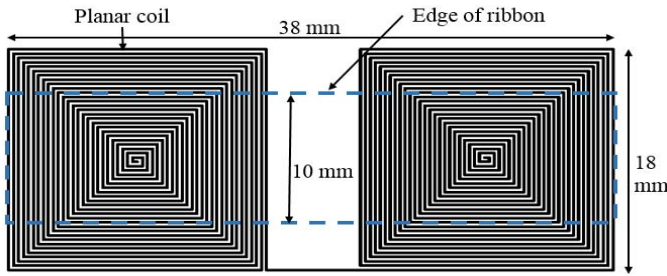


Fig. 1. Top view of the sensor, including planar coil design and ribbon.

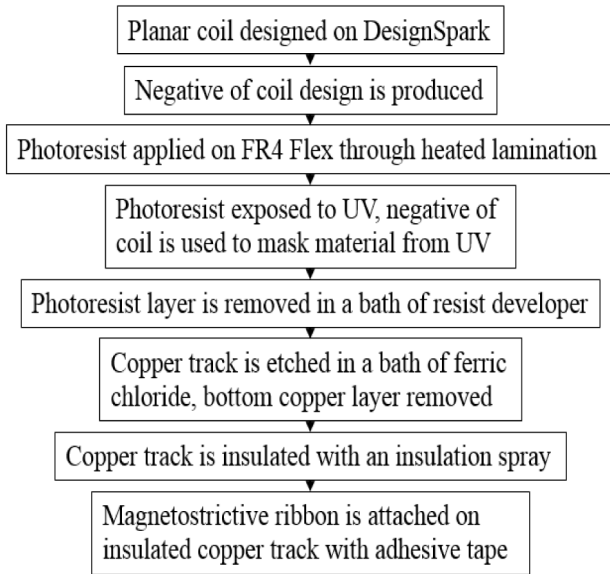


Fig. 2. Flowchart of the sensor fabrication process.

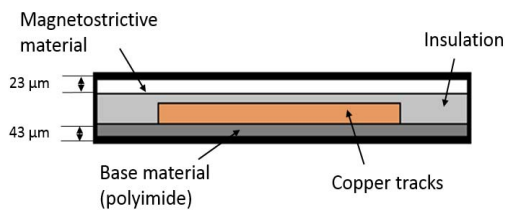


Fig. 3. Side profile of a track after etching (size not to scale).

the changes to the inductance value,  $L$ . The sensing element, Metglas 2605SA1, was chosen for its large magnetostriction, also for the flexibility of the ribbon.

To simulate bending motion, the sensor was attached on both ends to stationary weighted blocks, which were moved to create a bending effect on the sensor. Tensile stresses were induced in the magnetostrictive material due to the bending of the sensor, thus changing the permeability and the output signal of the oscillator. To measure the angle induced by the movement of the weighted ends, a mathematical model was used, which approximated the angles by using trigonometrical methods along with circle theorems. The model was used for an algorithm, shown in (1), which was written in LabView

$$\text{Curvature} = 180 - \left( 2 \times \sin^{-1} \left( 1 - \frac{x}{2y} \right) \right). \quad (1)$$

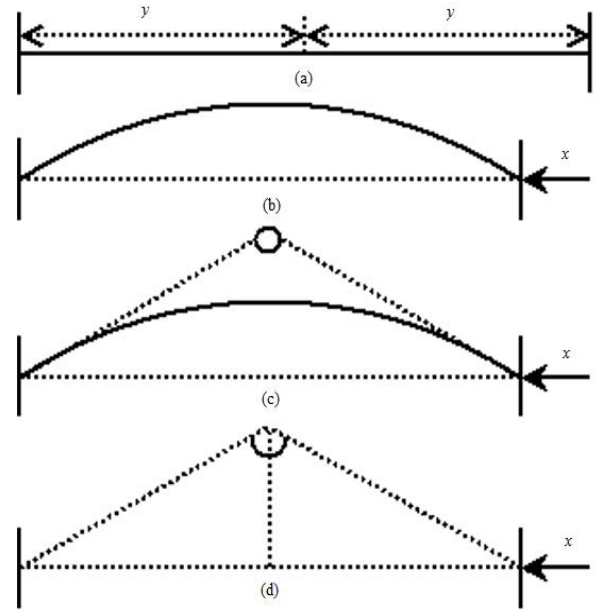


Fig. 4. Extrapolation of the angle from bending. (a) Sensor in relaxed state. (b) Sensor after the movement of distance  $x$ . (c) Extrapolation of parameters due to bending. (d) Estimation of the included angle induced.

The LabView program interprets the distance that the weight block was moved by into flexion angle induced, the model used for the approximation shown in Fig. 4.

The circuit was designed to oscillate at  $\sim 102$  kHz; however, the frequency was slightly above this as the inductance of the sensor was calculated using the planar inductor approximation calculations. This experiment will be referred to as experiment 1. The output signal was recorded as the movements induced bending in the sensor, and the distance traveled was converted into approximate degrees of bending in the sensor. The sensor starts at no distance traveled, where it is held taut and there is no bending, and it finishes at  $\sim 150^\circ$  curvature; this is approximately the maximum amount of bending, which is achievable with joints, such as the elbow and the knee. This ensures that the experimental results will represent the range of motion for most body joints. The experiment was repeated with different capacitors, to lower the oscillating frequency to  $\sim 40$  kHz, enabling comparison of the behavior of the sensor at different frequencies and to determine how the sensor performs in different operating conditions. This experiment will be referred to as experiment 2. The experiments were performed five times to ensure repeatability of the data obtained.

### III. RESULTS AND DISCUSSION

Fig. 5 shows the relationship between the changes of the output signal and the curvature. The frequency decreases by 4.44 kHz at maximum bending, which is a 4% difference compared with the oscillating frequency without bending. The amplitude of the signal increases by 0.43 V, and this is a 10% increase when compared with the oscillating signal's amplitude without bending.

The data shown in Fig. 6 display trends similar to that of Fig. 5, and the sensor is operating as intended in both

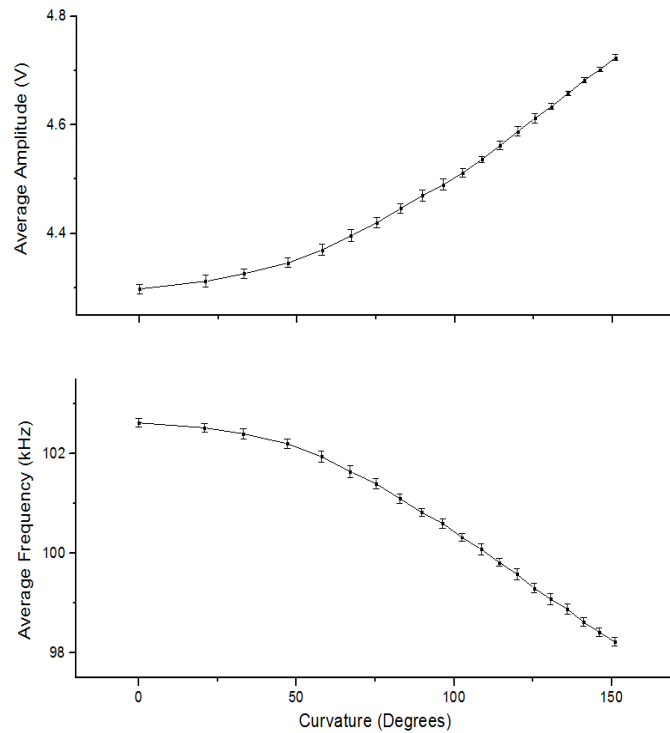


Fig. 5. Amplitude and frequency responses of the circuit at  $\sim 102$  kHz with standard deviation error bars.

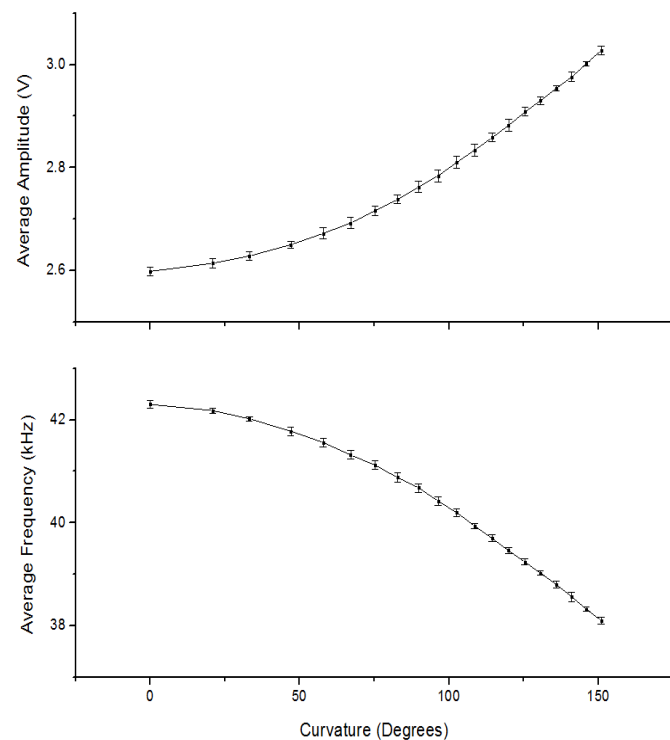


Fig. 6. Amplitude and frequency responses of the circuit at  $\sim 40$  kHz with standard deviation error bars.

operating conditions. The frequency shift caused by bending is 4.2 kHz at the maximum, and this difference caused by bending is 9.9% of the maximum oscillating frequency.

TABLE I  
MD FOR EXPERIMENT 1

Parameter	Mean Absolute Deviation
Frequency (Hz)	144.6
Amplitude (mV)	7.4

TABLE II  
MD FOR EXPERIMENT 2

Parameter	Mean Absolute Deviation
Frequency (Hz)	50.0
Amplitude (mV)	6.5

The amplitude of the signal increases by 0.43 V, and this is an increase in 16% from the maximum oscillating signal amplitude.

Both Figs. 5 and 6 show trends between the bending of the sensor and the shifts in the parameters of the output signal. The data show that the linearity of the response increases with the bending; however, at low degrees of bending, the response is not as linear. It can be seen on both Figs. 5 and 6 that the strong linearity begins after the bending exceeds  $50^\circ$ . This suggests that the low amount of stresses caused by minimal bending does not generate a large change to the output signals. Linearity measurements also show that the linearity of the data collected in both experiments are strong, whether it is measured across the whole curvature range or after the  $50^\circ$  point. The amplitude and the frequency of the output signal change with increased bending, allowing multiple methods of assessing the curvature of the sensor. FM and AM demodulation techniques are two examples, which can be used for signal processing purposes.

Statistical methods were used to analyze the data, to determine the mean absolute deviation (MD) of the collected data. The MD technique was used on both data sets, and the results were compared. Table I shows the data obtained from the MD analysis of experiment 1, where the oscillating frequency was set as 102 kHz. The results obtained show that the MD is low compared with the data obtained in experiment 1.

Table II shows that the deviation value is low for the both of the parameters, as the parameters of the signal produced in the experiments differed; the MD values did too accordingly. The mean absolute percentage error (MPE) was also calculated for both experiments, for experiment 1, the MPE for the frequency is 0.1%, and the MPE for the amplitude is 0.2%. The MPE for experiment 2 was calculated, and the MPE for the frequency is 0.1%, whereas the MPE for the amplitude is 0.2%.

The MD and MPE values obtained show that the results obtained from both experiments are tightly grouped, and this indicates that good repeatability was obtained from the sensor. The shift in the parameters of the output signal can be thought of as a scalar value, and it does not vary by much. This means that the sensor can be used in lower frequency oscillating circuits and/or oscillating circuits with low amplitudes and the results of bending the sensor will be largely significant. The difference in overall frequency change of 6% was achieved when the sensor's frequency was reduced, and this indicates that the sensor can be used in

different frequency ranges for differing applications without changing the sensor's fundamental design.

The experiments were conducted in the same environment. It is assumed that the earth's field may have some effect on the behavior of the magnetostrictive ribbon, but this was not investigated in this paper. No external bias field was applied to the sensor. Frequencies chosen for the experiments were selected to demonstrate the sensor's performance when operating at different frequencies, and the response of the sensor is shown to be similar for these two operating frequencies.

#### IV. CONCLUSION

The purpose of the sensor was to accurately track joint movements by relating curvature to flexion angle induced by the joint. This has been achieved as shown by the experimental results; the changes to the output signal caused by induced curvature can be measured, and repeatable results are obtained. The measurement uncertainty will be investigated further in the future studies where rigorous uncertainty analysis for the experiments will be undertaken. The size profile of the sensor is very miniscule, which is important for medical and virtual reality applications. Furthermore, the sensor produced exhibited strong linearity and great repeatability, which is encouraging for future works utilizing planar coil sensors.

The imitation of joint movement and the methods for extrapolating the flexion angle will be refined for future studies. Future investigations are planned to determine the response of the sensor over a larger frequency range. Heat treatment and prestressing are known methods for improving the performance of sensors utilizing amorphous materials, and this will be investigated in the future studies.

#### ACKNOWLEDGMENT

The authors would like to thank the Engineering and Physical Science Research Council for its support and studentship, without which this research would not have been possible. Information on how to access the data that support the results presented in the article can be found in the Cardiff University data catalog at <http://dx.doi.org/10.17035/d.2016.0008123122>.

#### REFERENCES

- [1] Y. Menguc *et al.*, "Soft wearable motion sensing suit for lower limb biomechanics measurements," in *Proc. IEEE Int. Conf. Robot. Autom. (ICRA)*, May 2013, pp. 5309–5316.
- [2] D. Son *et al.*, "Multifunctional wearable devices for diagnosis and therapy of movement disorders," *Nature Nanotechnol.*, vol. 9, no. 5, pp. 397–404, 2014.
- [3] H. Zeng and Y. Zhao, "Sensing movement: Microsensors for body motion measurement," *Sensors*, vol. 11, no. 1, pp. 638–660, 2011.
- [4] J. R. Windmiller and J. Wang, "Wearable electrochemical sensors and biosensors: A review," *Electroanalysis*, vol. 25, no. 1, pp. 29–46, 2013.
- [5] J.-Y. Kim and C.-H. Chu, "Analysis of energy consumption for wearable ECG devices," in *Proc. IEEE Sensors*, Nov. 2014, pp. 962–965.
- [6] P. Zhao, N. Deng, and Z. Wang, "Fabrication of ultra-thin silicon stress sensor chips with high flexibility and high sensitivity," in *Proc. IEEE Sensors*, Nov. 2014, pp. 1268–1271.
- [7] S. Yoon, J. K. Sim, and Y.-H. Cho, "On-chip flexible multi-layer sensors for Human stress monitoring," in *Proc. IEEE Sensors*, Nov. 2014, pp. 851–854.
- [8] T. Yamashita, Y. Zhang, H. Okada, T. Itoh, and R. Maeda, "Thin film based flexible current clamp sensor for green wireless sensor networks," in *Proc. IEEE Sensors*, Nov. 2014, pp. 742–745.
- [9] A. Eshkeiti *et al.*, "A novel self-supported printed flexible strain sensor for monitoring body movement and temperature," in *Proc. IEEE Sensors*, Nov. 2014, pp. 1615–1618.
- [10] I. Sasada, Y. Eto, and T. Kato, "A figure-of-eight flexible coil for a magnetostrictive torque sensor," in *Proc. IEEE Int. Magn. Conf. (INTERMAG)*, May 2006, p. 885.
- [11] A. T. Augousti, F.-X. Maletras, and J. Mason, "Improved fibre optic respiratory monitoring using a figure-of-eight coil," *Physiol. Meas.*, vol. 26, no. 5, pp. 585–590, 2005.